Downcore Variations of Sedimentary Detrital (238U/ 232Th) Ratio: Implications on the Use of 230Thxs and 231Paxs to Reconstruct Sediment Flux and Ocean Circulation

Lise Missiaen, S. Pichat, C. Waelbroeck, Éric Douville, L. Bordier, A. Dapoigny, François Thil, L. Foliot, Lukas Wacker

AGU100 ADVANCING EARTH AND SPACE SCIENCE

Geochemistry, Geophysics, Geosystems

RESEARCH ARTICLE
10.1029/2017GC007410

Key Points:
- The ($^{238}U/^{232}Th$) of the sediment detrital fraction of SU90-08 varied between 0.4 and 0.7 over the last 40 ky
- The influence of varying detrital ($^{238}U/^{232}Th$) value on widely used paleoceanographic proxies can exceed the uncertainty on the proxies
- The sensitivity to the detrital ($^{238}U/^{232}Th$) value mainly depends on the detrital fraction proportion and terrigenous material supply

Supporting Information:
- Supporting Information S1
- Data Set S1
- Data Set S2
- Data Set S3
- Data Set S4
- Data Set S5
- Data Set S5

Correspondence to:
L. Missiaen,
lise.missiaen@lsce.ipsl.fr

Citation:
Missiaen, L., Pichat, S., Waelbroeck, C., Douville, E., Bordier, L., Dapoigny, A., et al. (2018). Downcore variations of sedimentary detrital ($^{238}U/^{232}Th$) ratio: Implications on the use of $^{230}Th_{xs}$ and $^{231}Pa_{xs}$ to reconstruct sediment flux and ocean circulation. *Geochemistry, Geophysics, Geosystems*, *19*, 2560–2573. https://doi.org/10.1029/2017GC007410

Received 28 DEC 2017
Accepted 2 MAY 2018
Accepted article online 8 MAY 2018
Published online 17 AUG 2018

Downcore Variations of Sedimentary Detrital ($^{238}U/^{232}Th$) Ratio: Implications on the Use of $^{230}Th_{xs}$ and $^{231}Pa_{xs}$ to Reconstruct Sediment Flux and Ocean Circulation

L. Missiaen[1], S. Pichat[1,2,3], C. Waelbroeck[1], E. Douville[1], L. Bordier[1], A. Dapoigny[1], F. Thil[1], L. Foliot[1], and L. Wacker[4]

[1]Laboratoire des Sciences du Climat et de l'Environnement, LSCE/IPSL, CEA-CNRS-UVSQ-Université Paris-Saclay, Gif-sur-Yvette, France, [2]Laboratoire de Géologie de Lyon (LGL-TPE), ENS de Lyon, Université de Lyon, Lyon, France, [3]Climate Geochemistry Department, Max Planck Institute for Chemistry, Mainz, Germany, [4]Laboratory of Ion Beam Physics, ETH Zürich, Zürich, Switzerland

Abstract Excess ^{231}Pa and ^{230}Th ($^{231}Pa_{xs}$ and $^{230}Th_{xs}$) can be used to reconstruct past oceanic sedimentation (^{230}Th-normalized flux) and circulation changes ($(^{231}Pa/^{230}Th)_{xs,0}$, hereafter Pa/Th). These quantities are determined by computing the detrital and authigenic contributions from bulk sediment measurement. The method relies on the use of a chosen constant value of the detrital ($^{238}U/^{232}Th$) activity ratio (hereafter $(U/Th)_{det}$). In this study, we have extracted the detrital fraction of the sediments from North Atlantic deep-sea core SU90-08 (43°03′1N, 30°02′5W, 3,080 m) and determined its $(U/Th)_{det}$ value over the last 40 ky. We find that $(U/Th)_{det}$ varied significantly through time with a minimum value of 0.4 during the Holocene and a maximum value of 0.7 during the Last Glacial Maximum (LGM). The sensitivity of sedimentary ^{230}Th-normalized flux and Pa/Th is tested for our study site and for other North Atlantic sites. We show that the sensitivity is highly dependent on the core location and its terrigenous material supply. The ^{230}Th-normalized flux and Pa/Th signals are very robust in cores with low detrital contributions, whereas they are very sensitive to $(U/Th)_{det}$ changes in cores with higher detrital contribution. In the latter case, changes in ^{230}Th-normalized flux and Pa/Th due to the choice of a constant $(U/Th)_{det}$ can largely exceed the uncertainty on the ^{230}Th-normalized flux and Pa/Th, inducing potential biases in the amplitude and temporal variability of reconstructed sedimentation and ocean circulation changes.

1. Introduction

The U-series nuclides, and particularly ^{231}Pa, ^{230}Th, ^{232}Th, ^{238}U, provide a powerful tool to study oceanic processes such as sedimentation or circulation (Bacon & Anderson, 1982; Bourdon et al., 2003; Henderson & Anderson, 2003; Yu et al., 1996). For instance, ^{230}Th-normalization is now widely used to reconstruct past sedimentary fluxes and sedimentation rates (François et al., 1993, 2004; Winckler et al., 2016). Depending on the ocean basin considered, the sedimentary $(^{231}Pa/^{230}Th)_{xs,0}$ ratio (hereafter Pa/Th) enables to reconstruct past export productivity (Kumar et al., 1995; Pichat et al., 2004), or past overturning rates (Burckel et al., 2016; McManus et al., 2004; Yu et al., 1996).

Both proxies are based on the determination of the nuclides excess activities (subscript "xs") at the deposition time (subscript "0"). The excess activity corresponds to the fraction of the radioisotope that is produced in the water column by U decay and transferred to the sediment by adsorption on particles sinking in the water column. $^{230}Th_{xs,0}$ and $^{231}Pa_{xs,0}$ are calculated from bulk sediment measurements by correcting from the contribution of the detrital and authigenic fractions, and in situ decay of each radioisotope after deposition (François et al., 2004; Henderson & Anderson, 2003). Both the detrital and authigenic contributions to the measured concentration of the radioisotope are estimated based on several assumptions. The authigenic contribution corresponds to the radioisotopes produced by in situ radioactive decay of the parent authigenic U, accumulated under suboxic or anoxic conditions. It is calculated using decay constants of the parent isotope and the detrital contribution. This latter is itself derived from the terrigenous content of the sediment. In most previous studies the detrital contribution has been calculated using a chosen constant value for the ($^{238}U/^{232}Th$) activity ratio of the sediment detrital fraction (hereafter $(U/Th)_{det}$) (Table 1).

Table 1
Atlantic Literature $(U/Th)_{det}$ Values

References	$(U/Th)_{det}$ value	Region
Veiga-Pires and Hillaire-Marcel (1999)	0.58 ± 0.16	Labrador Sea
Thomson et al. (1999)	$0.7 \pm ?$	Iberian Margin
Henderson and Anderson (2003)	0.6 ± 0.1	Atlantic
McManus et al. (2004)	0.6 ± 0.2	N-Atlantic
Gherardi et al. (2009)	0.6 ± 0.1	N-Atlantic
Guihou et al. (2010)	0.5 ± 0.1	N-Atlantic
Bourne et al. (2012)	Local value (inferred from ^{234}U)	
Böhm et al. (2015)	0.47 ± 0.1	N-Atlantic
Burckel et al. (2016)	0.5 ± 0.1	Eq-Atlantic
Mulitza et al. (2017)	0.4 ± 0.03	Eq-Atlantic

There is actually no formal compilation of $(U/Th)_{det}$ in marine sediments and, for the Atlantic, the assumed $(U/Th)_{det}$ value and its uncertainty vary from one publication to another (Table 1). Regarding the choice of the $(U/Th)_{det}$ value, most authors used a constant value corresponding to a regional estimate as proposed in Henderson and Anderson (2003). For instance the value chosen for $(U/Th)_{det}$ was 0.6 in Gherardi et al. (2009), Henderson and Anderson (2003), and McManus et al. (2004) or 0.5 in Burckel et al. (2016) and Guihou et al. (2010). Others proposed to define local estimates of the $(U/Th)_{det}$ value. A first approach consists in using the average measured bulk ($^{238}U/^{232}Th$) (Veiga-Pires & Hillaire-Marcel, 1999). Later, Bourne et al. (2012) proposed a method to achieve a more precise estimate. ^{234}U is used as an indicator of the authigenic content and thus, enables to identify sediment levels characterized by an absence of authigenic contribution. In these levels, the measured bulk ($^{238}U/^{232}Th$) is used as the local estimate of $(U/Th)_{det}$. Finally, Böhm et al. (2015) and Mulitza et al. (2017) also attempted to use a local $(U/Th)_{det}$ estimate for their Pa/Th calculation and used, respectively, 0.47 and 0.4, corresponding to the minimum bulk ($^{238}U/^{232}Th$) of their records. They assumed that the minimum bulk ($^{238}U/^{232}Th$) value corresponds to depths where there is no authigenic contribution. Even though this approach provides a reliable upper limit for the local $(U/Th)_{det}$, it is not optimal since, in the absence of ^{234}U measurement, there is no conclusive evidence that there is no authigenic contribution at the considered levels. In addition, a temporal decreasing trend can be observed for the uncertainty associated to $(U/Th)_{det}$: while earlier studies used regional $(U/Th)_{det}$ estimates associated with relatively large uncertainties ± 0.2 (2σ) (Henderson & Anderson, 2003; McManus et al., 2004), more recent studies, still using basin-scale $(U/Th)_{det}$ estimate reduced the uncertainties to ± 0.1 (2σ) (Burckel et al., 2016; Gherardi et al., 2009; Guihou et al., 2010). Finally, the most recent study used a local estimate of $(U/Th)_{det}$, associated with an uncertainty of ± 0.03 (2σ) (Mulitza et al., 2017), i.e., more than 6 times smaller than the uncertainty used by the first studies cited above (Table 1).

Basin-scale variations in $(U/Th)_{det}$ have been reported. For instance, $(U/Th)_{det}$ has been shown to increase northward from 0.3 to 0.6 between 70°S and 45°S in the South Atlantic (Walter et al., 1997). In the equatorial Pacific, basin-scale variability has been considered (Anderson et al., 1983; Pichat et al., 2004). $(U/Th)_{det}$ values of 0.8 ± 0.2 were assumed in the east while 1.0 ± 0.3 was assumed for a core located close to Guinea based on a compilation of ($^{238}U/^{232}Th$) values of the potential detrital sources. Nevertheless, many Pa/Th studies involving cores from various Atlantic sites used a single $(U/Th)_{det}$ value (Gherardi et al., 2009; Guihou et al., 2010; Yu et al., 1996).

Overall, it is relevant to question whether the choice of the $(U/Th)_{det}$ value might significantly affect the records generated in those studies, which could be crucial when performing basin-wide or ocean-wide integrative studies based on the comparison of several records. Although some studies (Burckel et al., 2015; Lippold et al., 2016) have examined the impact of the choice of the $(U/Th)_{det}$ value on computed Pa/Th values, $(U/Th)_{det}$ has been assumed to be constant through time. However, ($^{238}U/^{232}Th$) depends on the geological nature and age of the parental material, resulting in highly variable ($^{238}U/^{232}Th$) at the Earth surface (supporting information Figure S1). The provenance of the detrital material or the relative contribution of various sources of detrital material can vary temporally, especially across climatic transitions. As shown by numerous studies, based on model experiments and/or paleoclimate proxies (Clement & Peterson, 2008; Hemming, 2004; Peterson et al., 2000; Voelker, 2002), rapid climate transitions are associated with changes

in precipitation regime, wind pattern, or iceberg discharge; hence, local changes in dust and/or riverine inputs, as well as ice rafted debris (IRD) are expected. It is thus likely that modifications in detrital inputs induce changes in the $(U/Th)_{det}$ value. Particularly in the case of locations characterized by high detrital inputs (for instance, coastal areas or areas subject to IRD discharges), changes in $(U/Th)_{det}$ can lead to substantial differences in the calculated $^{230}Th_{xs,0}$ and $^{231}Pa_{xs,0}$, and interpretation of associated proxies across climate transitions.

In this study, we investigate (i) the variations of $(U/Th)_{det}$ over the last 40 ky in a core located within the IRD Ruddiman belt in the North Atlantic and (ii) the effect of $(U/Th)_{det}$ changes on the computed ^{230}Th-normalized flux and Pa/Th, and on the interpretation of these proxies.

2. Materials and Methods

2.1. Core Location and Age Model

In order to study $(U/Th)_{det}$ variability through time, we sampled sediment core SU90-08 (43°03′1N, 30°02′5W, 3,080 m) located on the western flank of the Mid-Atlantic Ridge, within the Ruddiman belt (Figure 1). The sediment mainly consists in interbedded carbonates, foraminifera ooze, and mud (Bout-Roumazeilles et al., 1999). IRD layers containing coarse detrital material corresponding to Heinrich events 1, 2, and 4 are observed. Heinrich event 3 is not recorded in this core.

An age model has been previously established for core SU90-08 based on 10 radiocarbon dates covering the period from the Bolling-Allerod to Heinrich Stadial 4 (Vidal et al., 1997). Nevertheless, due to the core location (north of 40°N) and poorly constrained surface reservoir ages variations through the last glacial and the deglaciation (Bondevik et al., 2006; Waelbroeck et al., 2001), the age model cannot simply be derived from calibrated planktonic foraminifer ^{14}C ages beyond the Holocene. We thus constructed a new age model based on mixed pointers: ^{14}C dates for the Holocene period, where the reservoir ages are assumed to be constant and close to the current value of 400 ± 100 years, and alignment of sea surface temperature to Greenland air temperature for the glacial period (supporting information Table S1 and Figure S2). Planktonic foraminifera (*Globigerina bulloides*) were picked from four Holocene levels and radiocarbon dated using a Mini Carbon Dating System (MICADAS) with a gas introduction system (Fahrni et al., 2013; Wacker

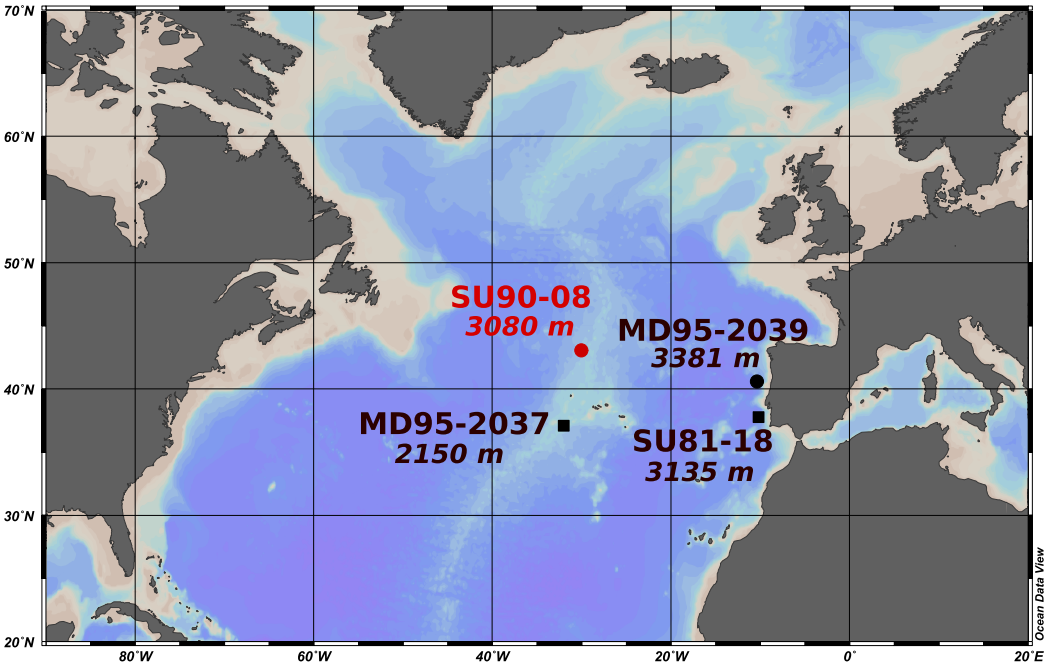

Figure 1. North Atlantic map showing the location of the cores used in this study. In red SU90-08 (new data: this study). In black, cores with published data: SU81-18 and MD95-2037 (Gherardi et al., 2009) and MD95-2039 (Thomson et al., 1999). Dots represent cores with U and Th data only; squares denote cores with U, Th, and Pa data.

et al., 2013) at Eidgenössiche Technische Hochscule Zürich (ETH-Zürich). The ^{14}C ages were calibrated to calendar ages using Oxcal (online version 4.3) (Ramsey, 2009), a reservoir age of 400 ± 100 years, and the IntCal13 calibration curve (Reimer et al., 2013). Deeper in the core, a new high-resolution sea surface temperature records (based on planktonic foraminifera assemblages (see supporting information text S1) and percentage of *Neogloboquadrina pachyderma* senestral) were aligned to North-GRIP $\delta^{18}O$, a proxy for air temperature above the ice sheet (Andersen et al., 2006; Bond et al., 1993; Rasmussen et al., 2006; Svensson et al., 2006; Vinther et al., 2006). The sedimentation rate was assumed to be constant between tie-points. More information about the methodology can be found in the supporting information (Cortijo et al., 1997; Therón et al., 2004; Waelbroeck et al., 1998).

2.2. ^{238}U and ^{232}Th Analysis in SU90-08 Detrital Fraction

In the following, parentheses denote activity or activity ratio. In order to determine as precisely as possible the $(^{238}U/^{232}Th)$ of the actual detrital fraction of the sediments (i.e., $(U/Th)_{det}$), we measured ^{238}U and ^{232}Th in different fractions of SU90-08 sediment samples: (i) we extracted the carbonate-free and ferromanganese-free sediment detrital fraction using a sequential leaching procedure, this fraction will be referred as the "leaching residue" in the following, (ii) we handpicked IRDs to analyze (a) bulk IRDs and (b) the detrital carbonates contained in the IRDs.

We used the sequential leaching procedure described in Pichat et al. (2014) to isolate the detrital fraction of the sediment from the carbonates and ferromanganese oxihydroxides. After the sequential leaching, the residue was digested in a mixture of concentrated HNO_3:HF (3:5 volume ratio) for 48 h at 150°C. The solution was then fumed with 2 mL $HClO_4$ at 170°C. During this procedure, beaker walls were rinsed 6 times with concentrated HNO_3. No residue was observed in the solutions after this digestion step. At near dryness, the sample was brought in 20 mL 2 N HNO_3. NH_4OH was added to precipitate Fe-oxyhydroxydes, which contain U and Th and leave the remaining fluorides in solution. The precipitate was washed 3 times with 18.2 MΩ water and finally dissolved in 5 mL 1 N HNO_3 and stored.

Because the leaching procedure removes carbonates, detrital carbonates possibly present in the sediment are also removed. However, it is known that IRDs have the potential to contain detrital carbonates (Hemming, 2004). To evaluate the impact of both IRDs and detrital carbonates contained in IRD layers on the sediment $(U/Th)_{det}$, we handpicked and measured $(^{238}U/^{232}Th)$ of (a) bulk IRDs and (b) IRD detrital carbonates. For that purpose, five levels with high IRD content were selected (see supporting information Figure S3). The bulk sediment was sieved and the coarse fraction (>150 μm) rinsed with deionized water and dried.

For bulk IRD analyses, individual detritic grains from different size fractions (>350, 350–250, 250–200, and 150–200 μm) were handpicked and mixed to obtain ca. 50 mg of material. The samples were digested in a mixture of concentrated HNO_3:HF (3:5, volume ratio) for 48 h at 150°C. The solution was then fumed with 2 mL $HClO_4$ at 170°C. During this procedure, beaker walls were rinsed 6 times with concentrated HNO_3.

For IRD detrital carbonates analyses, around 50 mg of individual detrital carbonate grains (from the same levels) were handpicked and dissolved in 0.5 N HCl for 4 h. After centrifugation, the supernatant (= carbonates) was isolated. The residue was further leached in 0.5 N HCl for 4 h and the supernatants were combined. The sample (supernatant or residue) was then fully digested in a mixture of concentrated HNO_3:HF and evaporated to dryness with frequent rinsing of the beaker walls by concentrated HNO_3 to ensure full removal of fluorides prior to analysis. The samples were then evaporated to near dryness, dissolved in 1 N HNO_3 and stored.

The quality of the chemistry was assessed by preparing procedural blanks along the sample treatment. The blanks were found to represent less than 1% of the samples signals.

Bulk IRDs and leaching residues $(^{238}U/^{232}Th)$ were diluted in 1 N HNO_3/0.01 N HF for analysis with addition of Re and In internal standards. The samples were measured using an Inductively Coupled Plasma Quadrupole Mass-Spectrometer (ICP-QMS, $X^{SeriesII}$ ThermoFisher) at the Laboratoire des Sciences du Climat et de l'Environnement (LSCE), France. The use of 1 N HNO_3/0.01 N HF carrier acid and of a PFA micronebulizer of 100 μL/min allowed rapid rinsing steps and high signal stability during measurements (signal variations represented about 1%) (Douville et al., 2010). U and Th concentrations were derived using an external calibration and corrected from the signal drift during the analysis using internal standard ^{185}Re monitoring. During the measurement sequence, ^{185}Re variations never exceeded 10% for the samples and 15% for home

standard solutions. The measurement quality and analytical uncertainties were controlled with reference materials SL-1 (sediment, International Atomic Energy Agency, Vienna), BR1 (basalt, CRPG, France) and GSR6 (carbonate rock, National Research Center for CRMs, China) dissolutions. The values obtained with this procedure agree with the certified or published values within the error bars (see supporting information Figure S4). The analytical uncertainties (2σ) do not exceed 8% on Th concentrations, 7% on U concentrations, and 2.5% on the ratio. The variability observed in our samples largely exceeds those uncertainties, with changes in samples Th concentration, U concentration, and (U/Th) ratio, respectively, 12.5, 14.3, and 40 times larger than the analytical errors (supporting information Tables S2 and S3).

^{238}U and ^{232}Th concentrations of both the carbonate and residual fractions from IRD detrital carbonates were measured by ICP-QMS (Agilent 7900 equipped with an ISIS 3 introduction system) at the Climate Geochemistry Department of the Max Planck Institute for Chemistry, Mainz, Germany (supporting information Tables S4 and S5). The accuracy of the measurement was assessed using slate OU-6. Both measured ^{232}Th and ^{238}U concentrations of OU-6 are within errors of the certified values (Kane, 2004). The precision of the measurement is 2% (2σ) for both the U and Th concentrations (supporting information Tables S4 and S5). As for the other Q-ICP-MS measurements, we used 2% HNO_3–0.01 N HF as acid carrier and a PFA nebulizer. Indium was used as internal standard to correct for instrumental drift.

To assess the leaching quality and efficiency, standard material BR1 was prepared in the same conditions as the samples. As this material is a basalt rock, the total ^{238}U and ^{232}Th content should end up in the residue fraction. We observed about ~22% loss of material (24% for Th and 20% for U) during the leaching steps most likely due to repeated transfers of the samples to different containers necessary to perform leaching and centrifugation steps (Pichat et al., 2014). However, the (^{238}U/^{232}Th) ratio of the BR1 standard was practically not affected and remained stable within 6% (2σ) uncertainties, taking into account the measurement error and the uncertainties deriving from element fractionation during the leaching procedure (supporting information Figure S4).

The reproducibility of the leaching residue measurements was assessed by replicate (^{238}U/^{232}Th) measurements of two samples (121 and 196 cm). The results differed by 2.5% and 1.4% at 121 and 196 cm, respectively, which is lower or equivalent to the analytical standard deviation (2.5%, 2σ) for simple digestion and lower than the analytical standard deviation for leaching preparation (6%, 2σ, assessed using BR1 standard preparation as explained above). To assess the sample preparation reproducibility as well as the potential sample heterogeneity, the full procedure was applied to 2 aliquots of the level 121 cm. Based on these aliquot measurements, we evaluated the external reproducibility (difference between the two measurements) to 10% (2σ).

2.3. ^{238}U, ^{230}Th, and ^{232}Th Analysis in SU90-08 Bulk Sediment

In order to investigate the potential impact of $(U/Th)_{det}$ change on the calculation of $^{230}Th_{xs}$, we measured radioisotope ^{230}Th, ^{232}Th, and ^{238}U activities in SU90-08 bulk sediment. The analyses were performed on 53 samples following the procedure of Guihou et al. (2010). The measurements were done by isotope-dilution mass-spectrometry on a MC-ICP-MS (Neptune^{Plus} Thermo Fisher) at LSCE, France.

2.4. ^{230}Th-Normalized Flux and Pa/Th Sensitivity to $(U/Th)_{Det}$ Variations

We conducted sensitivity tests to assess (1) the impact of $(U/Th)_{det}$ changes on the ^{230}Th-normalized flux and Pa/Th calculations and (2) the potential spatial variability of this impact. We used new data on core SU90-08 (this study) and published data from two cores located on the Iberian Margin: SU81-18 (37°46′N, 10°11′W, 3,135 m) (Gherardi et al., 2005) and MD95-2039 (40°34.71′N, 10°20.91′W, 3,381 m) (Thomson et al., 1999), and one core close to the Azores archipelago and the Mid-Atlantic Ridge: MD95-2037 (37°05′N, 32°01′W, 2,150 m) (Gherardi et al., 2009) (Figure 1). The age models used for the latter three cores are the ones of the original publications.

As explained in section 1, the calculation of the excess fraction of the measured total ^{230}Th and ^{231}Pa requires corrections from other ^{230}Th and ^{231}Pa sources (detrital and authigenic). This relies on the following assumptions. First, the ^{232}Th content of the sediment is assumed to be purely detrital. Then, detrital ^{230}Th is considered to be at secular equilibrium with detrital ^{238}U, i.e., $(^{238}U)_{det} = (^{230}Th)_{det}$. The incorporation of authigenic uranium occurs at the time of sediment deposition at a known (^{234}U/^{238}U) ratio, assumed to be

that of sea water: $(^{234}U/^{238}U)_{sw} = 1.1467$ ($1\sigma = 0.0025$) (Robinson et al., 2004). The equations used to determine Pa and Th excess activities are the following (Henderson & Anderson, 2003):

$$X_{xs} = X_{meas} - X_{det} - X_{auth} \quad (1)$$

where X stands for ^{231}Pa or ^{230}Th activities, "meas" for the measured activity, "det" for the detrital fraction, and "auth" for the authigenic fraction

$$^{230}Th_{xs} = {}^{230}Th_{meas} - \left(^{232}Th_{meas} \times (U/Th)det\right) - \left[{}^{238}U_{meas} - \left(^{232}Th_{meas} \times (U/Th)det\right) \times \left\{ \left(1 - e^{-\lambda 230 t}\right) + \frac{\lambda 230}{\lambda 230 - \lambda 234} \left(\left(\frac{234U}{238U}\right)_{sw} - 1 \right) \left(e^{-\lambda 234 t} - e^{-\lambda 230 t}\right) \right\} \right] \quad (2)$$

$$^{231}Pa_{xs} = {}^{231}Pa_{meas} - \left[\left(\frac{235U}{238U}\right)_{nat} \times (U/Th)det \times {}^{232}Th_{meas} \right] - \left[\left(\frac{235U}{238U}\right)_{nat} \times \left({}^{238}U_{meas} - (U/Th)det \times {}^{232}Th_{meas}\right) \times \left(1 - e^{-\lambda 231 t}\right) \right] \quad (3)$$

where λ_x is the decay constant of the considered isotope and t is the age of the sediment. $(^{235}U/^{238}U)_{nat} = 0.046$ is the natural activity ratio of U isotopes.

Finally, the excess fraction at the time of sediment deposition ($^{231}Pa_{xs,0}$, $^{230}Th_{xs,0}$) can be calculated by correcting $^{231}Pa_{xs}$ and $^{230}Th_{xs}$ from the radioactive decay:

$$(X)_{xs,0} = (X)_{xs}\, e^{\lambda x t} \quad (4)$$

The preserved vertical rain rate or ^{230}Th-normalized flux (in g m^{-2} yr^{-1}) of sediment is given by

$$\frac{Z \times \beta\ Th}{^{230}Th_{xs,0}}$$

where Z is the water depth at the core location in meters and β_{Th} is the production rate of ^{230}Th in the water column (= 0.0267 dpm m^{-3} yr^{-1}).

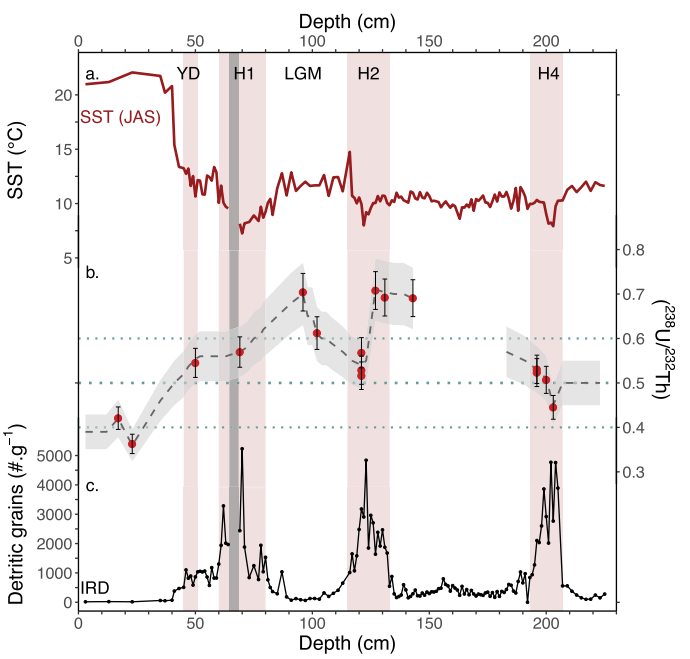

Figure 2. SU90-08 downcore variations. (a) Summer sea surface temperature (SST) reconstructed from planktonic foraminifera assemblages (see supporting information). (b) $(^{238}U/^{232}Th)$ of the leaching residues (red dots, see text section 2.2 for details) and associated standard deviation (2σ), interpolated $(U/Th)_{det}$ time series (dashed line) and associated uncertainty (2σ) (grey envelope). The dotted blue lines correspond to the most commonly used $(U/Th)_{det}$ and associated uncertainty. (c) Ice Rafted Debris content expressed as the number of >150 μm detritic grains per gram of dry sediment. The Younger Dryas and Heinrich layers are highlighted by red bands based on IRDs abundances. The vertical grey band corresponds to a sediment perturbation between 65 and 69 cm evidenced by reversals in ^{14}C ages as well as reversals in planktonic and benthic $\delta^{18}O$ and $\delta^{13}C$ signals. The data corresponding to the affected levels were systematically removed.

3. Results

3.1. Leaching Residues

The $(^{238}U/^{232}Th)$ ratio measured on SU90-08 leaching residues ranges from 0.36 ± 0.04 to 0.71 ± 0.07 (Figures 2 and 3, supporting information Table S2) and exhibits clear temporal variations. A major shift is observed between the Holocene period, where $(^{238}U/^{232}Th) \approx 0.4$, and the LGM period, where $(^{238}U/^{232}Th) \approx 0.7$. During the Younger Dryas (YD) and Heinrich events 1, 2, and 4, marked by relatively high IRD abundances, the $(^{238}U/^{232}Th)$ ratio is around 0.53, except for two points at the beginning of Heinrich layer 2. The observed temporal variations largely exceed the external reproducibility uncertainty (10%, 2σ) (Figure 2).

3.2. Handpicked Material

The $(^{238}U/^{232}Th)$ ratio of handpicked bulk IRDs and detrital carbonates is presented in Figure 3. Additionally, the maximal value of $(U/Th)_{det}$ was calculated assuming that the total measured ^{230}Th activity in the bulk sediment is of detrital origin, i.e., $(^{230}Th)_{meas} = (^{230}Th)_{det}$ (see equations (1) and (2)). The comparison of the sediment components $(^{238}U/^{232}Th)$ at a given depth (Figure 3) shows that (i) $(^{238}U/^{232}Th)$

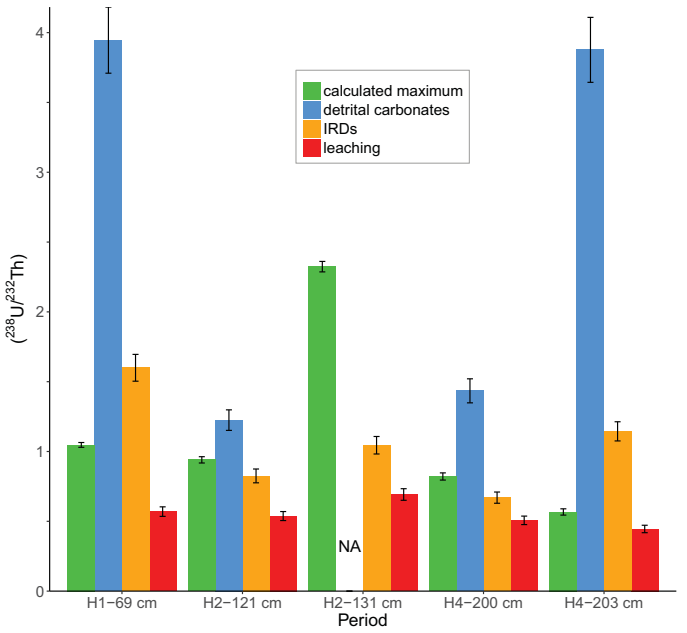

Figure 3. Comparison of the ($^{238}U/^{232}Th$) ratio measured in leaching residue (red) and handpicked material (bulk IRD (orange) and detrital carbonates (blue)) with calculated maximum $(U/Th)_{det}$ (green) for five IRD levels in SU90-08. The calculated maximum $(U/Th)_{det}$ was obtained from the total (^{230}Th) and (^{232}Th) activities under the hypothesis that the sediment is purely detrital (see equation (1)). The high calculated maximum $(U/Th)_{det}$ obtained at 131 cm compared to the other depths is due to the lower IRD abundance at that level. Consequently the proportion of the excess and/or authigenic fractions is larger at that level. "NA" stands for "not available": not enough detrital carbonates were found in level 131 cm to analyze the detrital carbonates ($^{238}U/^{232}Th$) signature.

measured in leaching residues is 2–9 times lower than that of detrital carbonates; (ii) the ($^{238}U/^{232}Th$) of bulk IRDs is up to 3 times higher than that of leaching residues; (iii) the detrital carbonate ($^{238}U/^{232}Th$) is always significantly higher than the calculated maximum $(U/Th)_{det}$.

4. Discussion

4.1. Constraining the Actual $(U/Th)_{det}$ Value

Figure 3 shows that the ($^{238}U/^{232}Th$) ratio measured in handpicked IRDs (i.e., detrital carbonates and bulk IRDs) is significantly different from the ($^{238}U/^{232}Th$) ratio measured in the leaching residues. Actually, none of the three measured components truly represents the detrital fraction of the sediment. Instead, we argue below that the ($^{238}U/^{232}Th$) of detrital carbonates on the one hand, and of leaching residues on the other hand, can be seen as end-members values bracketing the actual $(U/Th)_{det}$ value.

On the one hand, detrital carbonates only represent a part of the total sediment detrital fraction. On the other hand, the handpicked material (bulk IRDs and detrital carbonates) only represents the coarser fraction of the sediment (>150 μm), the finer fraction having been eliminated along the sieving step. The finer detrital fraction might indeed represent an important portion of the total sediment detrital fraction. Finally, the leaching residue contains the fine fraction but misses the detrital carbonates that are removed during the leaching procedure. Consequently, none of these three components is representative of the actual sediment detrital fraction. Additionally, it is important to note that none of the fractions measured in this study (bulk sediments, leaching residues, bulk IRDs, and detrital carbonates) present remarkably low (^{238}U) or (^{232}Th) activities compared to the other fractions (see supporting information Tables S2–S6). Therefore, it is not possible to conclude that one of these fractions would not significantly affect the actual ($^{238}U/^{232}Th$) of the true detrital fraction.

Detrital carbonates have systematically higher ($^{238}U/^{232}Th$) than the leaching residue (Figure 3). Thus, because the leaching residue misses the detrital carbonate fraction, the ($^{238}U/^{232}Th$) ratio measured on the leaching residues yields an underestimated detrital fraction ($^{238}U/^{232}Th$) value compared to the actual $(U/Th)_{det}$. Also, for a given depth, the ($^{238}U/^{232}Th$) ratio of the detrital carbonates is always much higher than the calculated maximum $(U/Th)_{det}$ (Figure 3). The calculated maximum $(U/Th)_{det}$ could be biased because it is determined on subsamples of only 200 mg that might not be representative of the total sample if the latter contains big IRD grains, like in the case of levels 200 and 203 cm. Despite this possible bias, the systematic and significant difference between the detrital carbonates ($^{238}U/^{232}Th$) and the calculated maximum $(U/Th)_{det}$ is consistent with the fact that detrital carbonates do not represent a large portion of the total detrital fraction. This is confirmed by the observation of levels 200 and 203 cm, which are characterized by very high IRD content (71% and 93% of the grains (foraminifera and IRDs) counted in the >150 μm size fraction, respectively). Examined under the binocular, these levels appeared to be almost entirely made of detrital material and contained very few foraminifera. For those levels, the leaching steps removed a very small fraction of the sediment, corresponding to biogenic (e.g., foraminifera) and detrital carbonates. For those levels, the leaching ($^{238}U/^{232}Th$) ratio is very close to the calculated maximum $(U/Th)_{det}$ and very different from the detrital carbonates ($^{238}U/^{232}Th$). Thus, detrital carbonates must represent a very small portion of the detrital fraction for the levels 200 and 203 cm. This is also the case for the rest of the core, as attested by the systematic and significant difference between the detrital carbonates and calculated maximum ($^{238}U/^{232}Th$). The low amount of detrital carbonates in the sediment is indeed consistent with the core location, relatively far from the sources of detrital carbonates (Andrews & Tedesco, 1992; Jennings et al., 2015). Consequently, our leaching residue ($^{238}U/^{232}Th$) measurements should be close to the actual $(U/Th)_{det}$ in SU90-08.

In cores with large detrital carbonate content (for instance cores closer to detrital carbonates sources), the leaching residue ($^{238}U/^{232}Th$) could be significantly lower than the actual $(U/Th)_{det}$ value. Consequently, the leaching residue ($^{238}U/^{232}Th$) could underestimate the actual $(U/Th)_{det}$ when the detrital carbonates represent an important part of the detrital fraction. In conclusion, the true $(U/Th)_{det}$ lies on a mixing line between detrital carbonates high ($^{238}U/^{232}Th$) and leaching residue low ($^{238}U/^{232}Th$) values. Moreover, in SU90-08, the true $(U/Th)_{det}$ should be close to the measured leaching residues ($^{238}U/^{232}Th$).

The range of ($^{238}U/^{232}Th$) values measured in SU90-08 leaching residues (Figure 2) is overall consistent with the ($^{238}U/^{232}Th$) values measured in the literature for the Atlantic basin (Veiga-Pires & Hillaire-Marcel, 1999; Walter et al., 1997). However, the downcore variability of leaching residue ($^{238}U/^{232}Th$) in SU90-08 (0.36 ± 0.04 to 0.71 ± 0.07) largely exceeds the $(U/Th)_{det}$ range assumed in the studies after 2004 (Table 1) that considered a constant $(U/Th)_{det}$ value and an error range ≤ 0.1 (2σ). Since the choice of $(U/Th)_{det}$ has the potential to affect the $^{231}Pa_{xs,0}$ and $^{230}Th_{xs,0}$ signals, variations of $(U/Th)_{det}$ with time could be considered, which has not been done in previous studies.

In conclusion, although the leaching residue misses the detrital carbonates, the leaching residue ($^{238}U/^{232}Th$) values are close (slightly underestimated) to the real $(U/Th)_{det}$ values because the detrital carbonates are representing only a small fraction of the total detrital fraction. Consequently, the ($^{238}U/^{232}Th$) range observed in the leaching residues of SU90-08 samples ($0.4–0.7 \pm 0.1$) is representative of the actual $(U/Th)_{det}$ range in these samples and a suitable basis for testing the sensitivity of excess fraction related proxies to $(U/Th)_{det}$ variations.

4.2. Impact of $(U/Th)_{det}$ Variations on the Estimation of Sedimentary Flux and Ocean Circulation Strength

We calculated the ^{230}Th-normalized flux (Figure 4) and Pa/Th ratio (Figure 5) using $(U/Th)_{det}$ values varying between 0.3 and 0.8, with a 0.1 increment, for the 4 cores presented in section 2.4 (Figure 1). For SU90-08, we compared these six ^{230}Th-normalized flux records with the ^{230}Th-normalized flux record obtained using a $(U/Th)_{det}$ value that varied with time as derived from leaching residue ($^{238}U/^{232}Th$) measurements (Figure 2b).

In order to calculate realistic uncertainties on the ^{230}Th-normalized flux and Pa/Th accounting for all sources of uncertainties, we performed Monte Carlo simulations (see supporting information text S2). In the two following sections, we assess whether changes in $(U/Th)_{det}$ can bias ^{230}Th-normalized fluxes or Pa/Th by comparing the uncertainty on ^{230}Th-normalized flux or Pa/Th ratio computed using Monte Carlo simulations with the range of variations in ^{230}Th-normalized flux or Pa/Th obtained using the two extreme $(U/Th)_{det}$ values of 0.3 and 0.8.

4.2.1. Assessing the Impact of $(U/Th)_{Det}$ Variations on ^{230}Th-Normalized Fluxes

We have identified three types of responses of the ^{230}Th-normalized flux to changes in $(U/Th)_{det}$ (Figure 4). Some cores are marginally affected, as exemplified by core MD95-2037 near the Azores, where an increase of $(U/Th)_{det}$ from 0.3 to 0.8 leads to a minor 6.6% increase of the ^{230}Th-normalized flux (median value) over the length of the record. The second type of behavior corresponds to cores for which the ^{230}Th-normalized flux is significantly affected by $(U/Th)_{det}$ changes only during specific time periods as illustrated by core SU90-08, near the Mid-Atlantic Ridge, where the ^{230}Th-normalized flux is mainly affected during Heinrich events. The major part of the downcore record displays a limited 18.1% (median of all values) increase in ^{230}Th-normalized flux when applying an increase in $(U/Th)_{det}$ from 0.3 to 0.8. In contrast, within Heinrich layers, the ^{230}Th-normalized flux is, on average, multiplied by almost 3. Finally, the ^{230}Th-normalized flux record can be significantly affected by $(U/Th)_{det}$ changes along the entire core as exemplified by the two Iberian margin cores, SU81-18 and MD95-2039. In these cores, the ^{230}Th-normalized flux record is homogeneously affected, with a median increase in the ^{230}Th-normalized flux of 65% and 61% for SU81-18 and MD95-2039, respectively, in response to an increase from 0.3 to 0.8 in $(U/Th)_{det}$.

The standard deviation (2σ) for the ^{230}Th-normalized flux calculated following the Monte Carlo simulation varies between the cores. For the Iberian margin cores, the average relative error ranges from 12.2% (SU81-18) to 14.4% (MD95-2039). For the Mid-Atlantic Ridge cores, it is $\sim$3% for MD95-2037 and 4.3% for SU90-08, but it becomes much larger (19% on average) in Heinrich layers for the latter. For Mid-Atlantic Ridge core MD95-2037, the small change in ^{230}Th-normalized flux in response to an increase in $(U/Th)_{det}$ from 0.3 to 0.8 (6%) corresponds to only twice the Monte Carlo error. Therefore, in cases similar to MD95-2037, a poorly

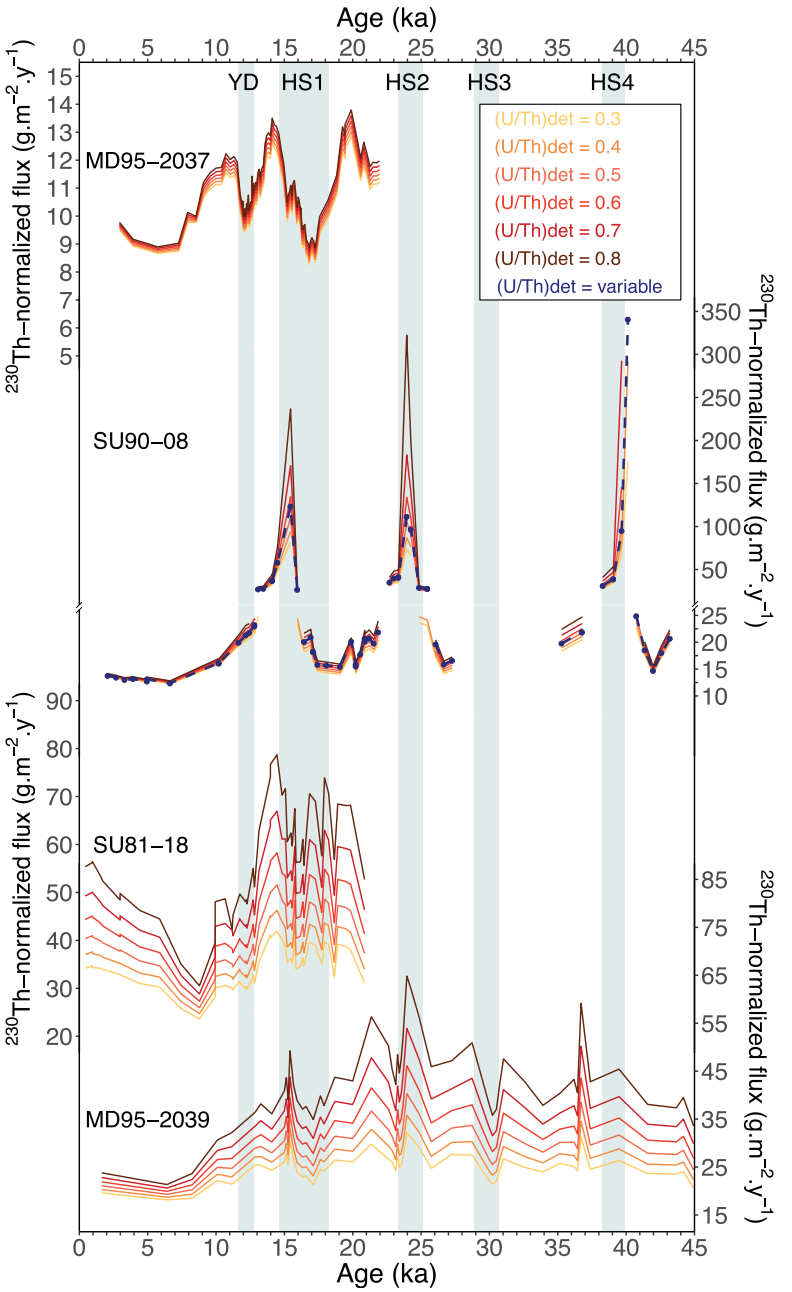

Figure 4. Sensitivity of ^{230}Th-normalized flux to $(U/Th)_{det}$ variations. The variable $(U/Th)_{det}$ corresponds to the $(U/Th)_{det}$ time series presented in Figure 2. Grey bands delineate the YD and Heinrich stadials chronozones. For SU90-08 we note that in HS4, there are missing ^{230}Th-normalized flux values for $(U/Th)_{det}$ = 0.7 and 0.8. For these data points, the calculation with high $(U/Th)_{det}$ values gives computed detrital fractions above 100%. As this is physically impossible, these data points were removed (see supporting information Figure S6).

constrained $(U/Th)_{det}$ value does not enlarge too much the error on the ^{230}Th-normalized flux, the uncertainty being kept below 10%. In contrast, for Iberian margin cores (SU81-18, MD95-2039), an increase in $(U/Th)_{det}$ from 0.3 to 0.8 leads to a ~60% increase in ^{230}Th-normalized flux. This change largely exceeds the Monte Carlo error on the ^{230}Th-normalized flux (~14%). The same conclusion is valid for SU90-08, especially in Heinrich layers where the ^{230}Th-normalized flux can be multiplied by 2–3 in response to an increase from 0.3 to 0.8 in the $(U/Th)_{det}$. Thus, in SU90-08, knowing the $(U/Th)_{det}$ is necessary to correctly evaluate the increase in ^{230}Th-normalized flux during the Heinrich events (Figure 4).

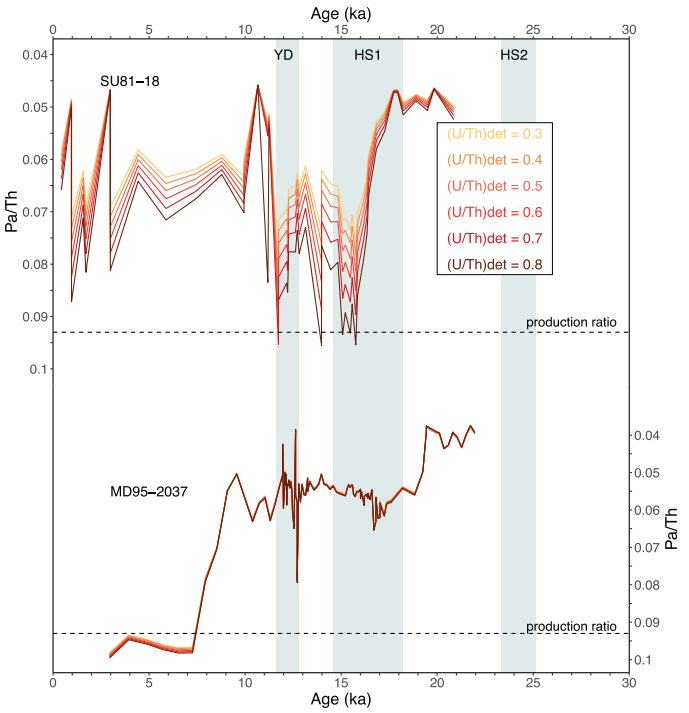

Figure 5. Sensitivity of Pa/Th to $(U/Th)_{det}$ variations. $(U/Th)_{det}$ values and grey bands as in Figure 4.

In the cases where the $(U/Th)_{det}$ is not well constrained, the consequences of the choice of a $(U/Th)_{det}$ value must be carefully examined. For example, assuming that the $(U/Th)_{det}$ variability in Iberian Margin cores is comparable to that observed in SU90-08, the ^{230}Th-normalized flux would decrease from roughly 65 to 45 g m^{-2} yr^{-1} for SU81-18, and from 45 to 30 g m^{-2} yr^{-1} for MD95-2039, from 17 to 10 ka. In both cases, it would correspond to a 30% decrease in ^{230}Th-normalized flux, with potential consequences on all the quantities derived from the ^{230}Th-normalized flux value, such as mass accumulation or sedimentation rates.

4.2.2. Assessing the Impact of $(U/Th)_{det}$ Variations on Pa/Th

For Pa/Th, we also observe different responses to changes in $(U/Th)_{det}$ (Figure 5). Mid-Atlantic Ridge core MD95-2037 shows almost no Pa/Th variations—on average 1%—for a $(U/Th)_{det}$ varying between 0.3 and 0.8. The latter Pa/Th variation is lower than the uncertainty calculated by Monte Carlo ($2\sigma = 6.5\%$). Iberian Margin core SU81-18 shows an overall greater sensitivity to $(U/Th)_{det}$ changes with an average Pa/Th variation of 15.5% for a 0.3–0.8 increase in $(U/Th)_{det}$. However, while some parts of the record, such as the LGM, only display minor (3.4%) variations, other sections, such as the Heinrich Stadial 1 (HS1), vary by up to 25%. The uncertainty on Pa/Th, calculated by Monte Carlo simulations is about 14% on average for core SU81-18. Thus, the change in Pa/Th due to variations in $(U/Th)_{det}$ is about twice as big as the uncertainty on Pa/Th for this core. Consequently, an improper estimation of the $(U/Th)_{det}$ value could lead to a misevaluation of the Pa/Th increase during HS1, interpreted as circulation slowdown (Gherardi et al., 2009). For example, assuming a constant $(U/Th)_{det}$ value of 0.7 (i.e., SU90-08 glacial value), Pa/Th would vary from 0.05 at the LGM to 0.085 during the Holocene, whereas assuming a $(U/Th)_{det}$ of 0.4 (i.e., SU90-08 Holocene value), Pa/Th would vary from 0.05 to 0.075 over the same interval. More importantly, a change of the $(U/Th)_{det}$ value through time could actually result in a bigger amplitude of the Pa/Th change or, conversely, could damp or erase the temporal variability of the Pa/Th signal obtained using a constant $(U/Th)_{det}$ value. For instance, a shift of $(U/Th)_{det}$ from 0.4 to 0.8 at the end of HS1 in Iberian Margin core SU81-18 would erase the increase in overturning rate at the end of HS1 that is derived from Pa/Th measurements when assuming a constant $(U/Th)_{det}$ value.

Interestingly, for both cores, Pa/Th is less affected than the ^{230}Th-normalized flux. Indeed, in core MD95-2037, Pa/Th is virtually not affected by changes in the $(U/Th)_{det}$ value. In SU81-18, the Pa/Th record is little affected over some time periods, such as the LGM or the late Holocene, while much larger Pa/Th variations (0.02–0.03) are calculated over other time periods, such as 16–11 ka (Figure 5). In contrast, the ^{230}Th-normalized flux record in SU81-18 is affected by $(U/Th)_{det}$ variations to a similar extent over its entire length. The lower sensitivity of Pa/Th compared to the ^{230}Th-normalized flux can be explained by the fact that the detrital correction affects both the Pa_{xs} and Th_{xs} calculations and thus partially cancels out in the Pa/Th calculation despite the different corrections applied for the two isotopes (see equations (2) and (3)).

4.3. Controls on $^{230}Th_{xs}$ and $^{231}Pa_{xs}$ Sensitivity to $(U/Th)_{Det}$

We have shown that the ^{230}Th-normalized flux and Pa/Th records do not exhibit the same sensitivity to changes in $(U/Th)_{det}$ in different cores. Here we discuss the impact of the core location (water depth, coastal area versus open ocean) and nature of the terrigenous supply (e.g., IRD contribution, river inputs, etc.) on this sensitivity.

^{230}Th-normalized flux and Pa/Th are calculated using excess ^{231}Pa and ^{230}Th, i.e., the ^{231}Pa and ^{230}Th produced in the water column and scavenged to the sediment. Consequently, one should expect the deeper cores to have a larger proportion of $^{231}Pa_{xs}$ and $^{230}Th_{xs}$ for a given detrital contribution because the water column is thicker; hence, more excess is produced. Among the studied cores, MD95-2037 is the least sensitive to the changes in $(U/Th)_{det}$ value although it is the shallowest (2,150 m). Thus, the water depth itself

does not seem to be the dominating factor controlling the ^{230}Th-normalized flux and Pa/Th sensitivity to $(U/Th)_{det}$ at the studied locations.

MD95-2037 is the core the most remote from terrigenous inputs. This is confirmed by the relatively high (^{230}Th) activity compared to (^{232}Th) activity. Indeed, it is located very far from the coasts and is consequently not significantly affected by riverine input (Figure 1). It is also too far south to receive notable IRD inputs. This is illustrated by the fact that for a given $(U/Th)_{det}$, the total calculated detrital contribution, X_{det} (equation (1)), does not exceed 10% of the measured (^{230}Th) or (^{231}Pa) signals (Figure 6). For MD95-2037, the dominant fraction is the excess fraction (Figure 6), which explains the low sensitivity of the data to the value of $(U/Th)_{det}$.

Core SU90-08 is also located far from the coasts and thus receives negligible riverine inputs. However, this core is located within the Ruddiman belt, so that its detrital content is highly influenced by IRD deposits during Heinrich events. The calculated detrital contribution for (^{230}Th) varies between 15% and 18% of the measured signal outside of the Heinrich layers but reaches 45%, 55%, and 90% during HS1, HS2, and HS4, respectively (Figure 6). Overall, in Heinrich layers, because of the significant increase of the detrital content, the excess fraction is greatly reduced and consequently, the detrital correction becomes very important. Therefore, it is critical to evaluate the $(U/Th)_{det}$ value in Heinrich layers to assess the correct detrital correction. Moreover, in the detrital-rich levels, the uncertainty on $^{230}Th_{xs}$ or $^{231}Pa_{xs}$ increases because the detrital and authigenic corrections are larger (equations (2) and (3)). In some cases, the uncertainties on $^{230}Th_{xs}$ or $^{231}Pa_{xs}$ calculations can be very large such as at 203 cm, where the calculated 2σ uncertainty on the ^{230}Th-normalized flux reached 42% (supporting information Figure S5). This data point is very uncertain but consistent with the rest of the record and should be considered with particular care in subsequent paleoceanographic interpretations.

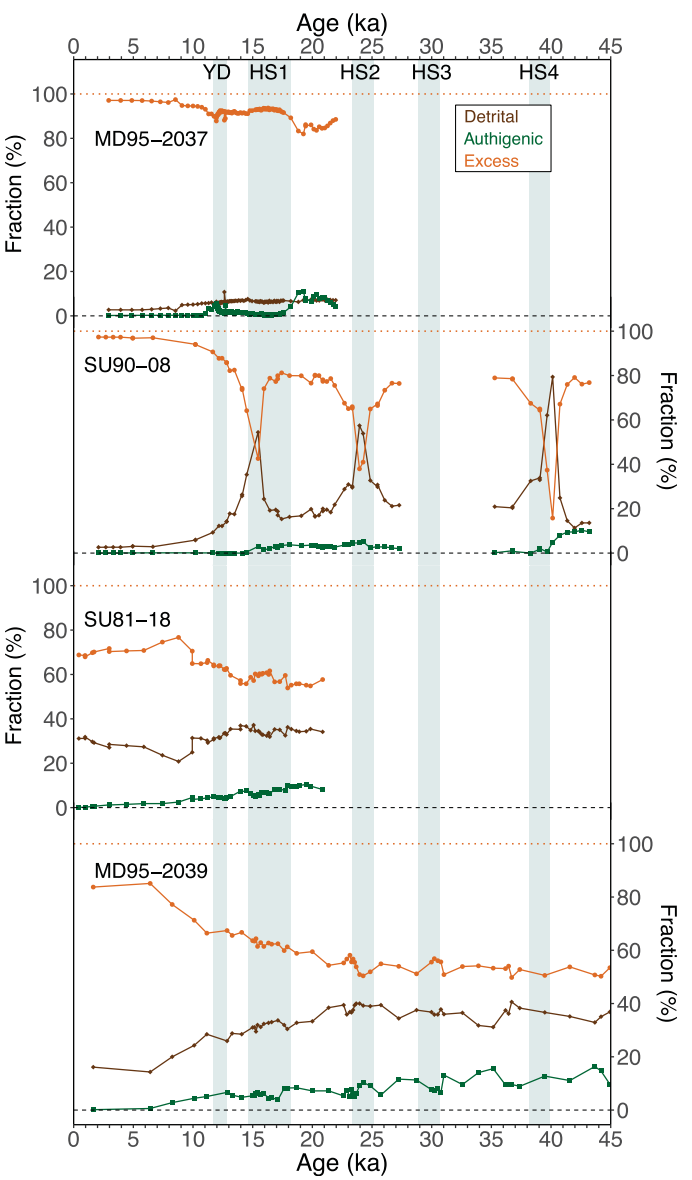

Figure 6. Computed detrital, authigenic, and excess fractions (%) for the studied cores. The fractions are computed based on equation (2). The results shown here are obtained for $(U/Th)_{det} = 0.5$ for MD95-2037, MD95-2039, and SU81-18. For SU90-08, we used $(U/Th)_{det}$ values based on our measurements as shown in Figure 2. The grey bands are as in Figures 4 and 5.

Finally, Iberian margin cores SU81-18 and MD95-2039 likely receive significant riverine or even Saharan dust inputs, as shown by average detrital contribution of 30% and 35% for SU81-18 and MD95-2039, respectively (Figure 6). In these two cores, the detrital contribution seems to have been roughly constant throughout the entire records as highlighted by a roughly constant (^{230}Th/^{232}Th) of about 1.5 downcore. This might not always be the case for all coastal records and we strongly recommend to evaluate the effect of potential detrital inputs temporal variations in coastal cores or cores strongly influenced by mineral aerosols inputs.

5. Conclusions

We have examined the influence of the sediment detrital fraction (^{238}U/^{232}Th) activity ratio, $(U/Th)_{det}$, on the calculation of two proxies that are widely used for the reconstruction of past oceanic sedimentation (^{230}Th-normalized flux) and circulation (Pa/Th) changes. We have shown that the $(U/Th)_{det}$ value varied between 0.4 and 0.7 in North Atlantic core SU90-08 over the last 40 ky. The largest measured $(U/Th)_{det}$ change was observed across the deglaciation, with values ranging from 0.7 at the LGM, to 0.4 during the Holocene. Therefore, considering a chosen constant $(U/Th)_{det}$ value associated with a ± 0.1 uncertainty (2σ), as commonly done in Pa/Th and ^{230}Th-normalized studies, cannot account for the variability observed in SU90-08.

The sensitivity of $^{230}Th_{xs}$ and $^{231}Pa_{xs}$ to changes in $(U/Th)_{det}$ was tested for core SU90-08 and three additional cores from the North

Atlantic. We find that both ^{230}Th-normalized flux and Pa/Th can be sensitive to changes in $(U/Th)_{det}$ for some core locations and that this sensitivity is highly dependent on the terrigenous inputs in the considered area. For cores located in the open ocean, far from riverine inputs, and away from the influence of iceberg discharges, the terrigenous fraction represents a small proportion of the sediments, thus changes in the estimate of the $(U/Th)_{det}$ have little impact on $^{230}Th_{xs}$ and $^{231}Pa_{xs}$. For shallow cores located close continental margins or affected by ice rafting, the detrital fraction may represent 30–90% of the signal, thus the ^{230}Th-normalized flux and Pa/Th records are much more affected by changes in the $(U/Th)_{det}$ value. For those cores, the changes in ^{230}Th-normalized flux due to the choice of a constant $(U/Th)_{det}$ value can largely exceed the uncertainty on the ^{230}Th-normalized flux. For some specific time periods, the same conclusion applies for Pa/Th. Our study shows that in some cases, misestimating $(U/Th)_{det}$ can lead to a misinterpretation of the amplitude of sediment fluxes or circulation changes. In other cases, if the temporal variations of $(U/Th)_{det}$ are not taken into account, the temporal variability of sediment fluxes or circulation changes may not be correctly reconstructed. In both cases, misevaluating $(U/Th)_{det}$ can be critical when comparing different cores and reconstructing regional or basin-scale changes in ocean circulation.

In conclusion, when using $^{231}Pa_{xs}$ and/or $^{230}Th_{xs}$ it is recommended to (i) assess the relative proportion of the detrital contribution at the studied locations, (ii) consider potential temporal variations of the $(U/Th)_{det}$, especially when the choice of this value has large effects on $^{230}Th_{xs}$ or $^{231}Pa_{xs}$, (iii) use uncertainties for $(U/Th)_{det}$ not lower than the $(U/Th)_{det}$ measurement external reproducibility, and (iv) evaluate the error on $^{231}Pa_{xs}$ and $^{230}Th_{xs}$ accounting for the uncertainty on the $(U/Th)_{det}$ value at the studied location. Future work is necessary to measure $(U/Th)_{det}$ in cores from different regions and evaluate the impact of $(U/Th)_{det}$ on Pa/Th and ^{230}Th-normalized flux records obtained in these different regions. It would also be of great interest to explore the potential of monitoring $(U/Th)_{det}$ temporal variations using routine measurements such as mineral characterization, major, and/or trace elements analysis.

Data availability

The data are given as Tables S1–S6 in the supporting information and are available online on Pangaea database (https://doi.pangaea.de/10.1594/PANGAEA.889695).

Competing interests

The authors declare that they have no conflict of interests.

References

Andersen, K. K., Svensson, A., Johnsen, S. J., Rasmussen, S. O., Bigler, M., Röthlisberger, R., et al. (2006). The Greenland ice core chronology 2005, 15–42 ka. Part 1: Constructing the time scale. *Quaternary Science Reviews*, *25*(2324), 3246–3257.

Anderson, R. F., Bacon, M. P., & Brewer, P. G. (1983). Removal of ^{230}Th and ^{231}Pa at ocean margins. *Earth and Planetary Science Letters*, *66*, 73–90.

Andrews, J., & Tedesco, K. (1992). Detrital carbonate-rich sediments, northwestern Labrador Sea: Implications for ice-sheet dynamics and iceberg rafting (Heinrich) events in the North Atlantic. *Geology*, *20*(12), 1087–1090.

Bacon, M. P., & Anderson, R. F. (1982). Distribution of thorium isotopes between dissolved and particulate forms in the deep sea. *Journal of Geophysical Research*, *87*(C3), 2045–2056. https://doi.org/10.1029/JC087iC03p02045

Böhm, E., Lippold, J., Gutjahr, M., Frank, M., Blaser, P., Antz, B., et al. (2015). Strong and deep Atlantic meridional overturning circulation during the last glacial cycle. *Nature*, *517*(7532), 73–76.

Bond, G., Broecker, W., Johnsen, S., McManus, J., Labeyrie, L., Jouzel, J., et al. (1993). Correlations between climate records from North Atlantic sediments and Greenland ice. *Nature*, *365*(6442), 143–147.

Bondevik, S., Mangerud, J., Birks, H. H., Gulliksen, S., & Reimer, P. (2006). Changes in North Atlantic radiocarbon reservoir ages during the Allerød and Younger Dryas. *Science*, *312*(5779), 1514–1517.

Bourdon, B., Turner, S., Henderson, G. M., & Lundstrom, C. C. (2003). Introduction to U-series geochemistry. *Reviews in Mineralogy and Geochemistry*, *52*(1), 1–21. https://doi.org/10.2113/0520001

Bourne, M. D., Thomas, A. L., Mac Niocaill, C., & Henderson, G. M. (2012). Improved determination of marine sedimentation rates using. *Geochemistry, Geophysics, Geosystems*, *13*, Q09017. https://doi.org/10.1029/2012GC004295

Bout-Roumazeilles, V., Cortijo, E., Labeyrie, L., & Debrabant, P. (1999). Clay mineral evidence of nepheloid layer contributions to the Heinrich layers in the northwest Atlantic. *Palaeogeography, Palaeoclimatology, Palaeoecology*, *146*(1–4), 211–228.

Burckel, P., Waelbroeck, C., Gherardi, J. M., Pichat, S., Arz, H., Lippold, J., et al. (2015). Atlantic Ocean circulation changes preceded millennial tropical South America rainfall events during the last glacial. *Geophysical Research Letters*, *42*, 411–418. https://doi.org/10.1002/2014GL062512

Burckel, P., Waelbroeck, C., Luo, Y., Roche, D. M., Pichat, S., Jaccard, S. L., et al. (2016). Changes in the geometry and strength of the Atlantic meridional overturning circulation during the last glacial (20–50 ka). *Climate of the Past*, *12*(11), 2061.

Acknowledgments

This is a contribution to ERC project ACCLIMATE; the research leading to these results has received funding from the European Research Council under the European Union's Seventh Framework Programme (FP7/2007–2013)/ERC grant agreement 339108. The authors thank J. Duprat for planktonic foraminifer census counts; M. Roy-Barman for expert advice on radioisotope measurements on LSCE MC-ICP-MS; and S. Moreira for his help with R programming. S. Pichat was supported by a research sabbatical (CRCT) from the ENS de Lyon. S. Pichat is thankful to S.J.G. Galer for allowing him to use the Max Planck Institute Q-ICP-MS and to K.P. Jochum for his help with standard reference material. This is LSCE contribution 6412.

Clement, A. C., & Peterson, L. C. (2008). Mechanisms of abrupt climate change of the last glacial period. *Reviews of Geophysics*, *46*, RG4002. https://doi.org/10.1029/2006RG000204

Cortijo, E., Labeyrie, L., Vidal, L., Vautravers, M., Chapman, M., Duplessy, J.-C., et al. (1997). Changes in sea surface hydrology associated with Heinrich event 4 in the North Atlantic Ocean between 40 and 60 N. *Earth and Planetary Science Letters*, *146*(1–2), 29–45.

Douville, E., Sallé, E., Frank, N., Eisele, M., Pons-Branchu, E., & Ayrault, S. (2010). Rapid and accurate U-Th dating of ancient carbonates using inductively coupled plasma-quadrupole mass spectrometry. *Chemical Geology*, *272*(1–4), 1–11. https://doi.org/10.1016/j.chemgeo.2010.01.007

Fahrni, S., Wacker, L., Synal, H.-A., & Szidat, S. (2013). Improving a gas ion source for ^{14}C AMS. *Nuclear Instruments and Methods in Physics Research Section B*, *294*, 320–327.

François, R., Bacon, M. P., Altabet, M. A., & Labeyrie, L. D. (1993). Glacial/interglacial changes in sediment rain rate in the SW Indian sector of subantarctic waters as recorded by ^{230}Th, ^{231}Pa, U, and δ^{15}N. *Paleoceanography*, *8*(5), 611–629. https://doi.org/10.1029/93PA00784

François, R., Frank, M., Rutgers van der Loeff, M. M., & Bacon, M. P. (2004). ^{230}Th normalization: An essential tool for interpreting sedimentary fluxes during the late Quaternary. *Paleoceanography*, *19*, PA1018. https://doi.org/10.1029/2003PA000939

Gherardi, J. M., Labeyrie, L., McManus, J. F., Francois, R., Skinner, L. C., & Cortijo, E. (2005). Evidence from the Northeastern Atlantic basin for variability in the rate of the meridional overturning circulation through the last deglaciation. *Earth and Planetary Science Letters*, *240*(3–4), 710–723. https://doi.org/10.1016/j.epsl.2005.09.061

Gherardi, J. M., Labeyrie, L., Nave, S., Francois, R., McManus, J. F., & Cortijo, E. (2009). Glacial-interglacial circulation changes inferred from ^{231}Pa/^{230}Th sedimentary record in the North Atlantic region. *Paleoceanography*, *24*, PA2204. https://doi.org/10.1029/2008PA001696

Guihou, A., Pichat, S., Nave, S., Govin, A., Labeyrie, L., Michel, E., et al. (2010). Late slowdown of the Atlantic Meridional Overturning Circulation during the last glacial inception: New constraints from sedimentary (^{231}Pa/^{230}Th). *Earth and Planetary Science Letters*, *289*(3–4), 520–529.

Hemming, S. R. (2004). Heinrich events: Massive late Pleistocene detritus layers of the North Atlantic and their global climate imprint. *Reviews of Geophysics*, *42*, RG1005. https://doi.org/10.1029/2003RG000128

Henderson, G. M., & Anderson, R. F. (2003). The U-series toolbox for paleoceanography. *Reviews in Mineralogy and Geochemistry*, *52*(1), 493–531. https://doi.org/10.2113/0520493

Jennings, A., Andrews, J., Pearce, C., Wilson, L., & Ólfasdóttir, S. (2015). Detrital carbonate peaks on the Labrador shelf, a 13–7 ka template for freshwater forcing from the Hudson Strait outlet of the Laurentide Ice Sheet into the subpolar gyre. *Quaternary Science Reviews*, *107*(Suppl. C), 62–80. https://doi.org/10.1016/j.quascirev.2014.10.022

Kane, J. S. (2004). Report of the International Association of Geoanalysts on the Certification of Penrhyn Slate, OU-6. *Geostandards and Geoanalytical Research*, *28*(1), 53–80.

Kumar, N., Anderson, R. F., Mortlock, R. A., Froelich, P. N., Kubik, P., Dittrich-Hannen, B., et al. (1995). Increased biological productivity and export production in the glacial Southern Ocean. *Nature*, *378*(6558), 675.

Lippold, J., Gutjahr, M., Blaser, P., Christner, E., de Carvalho Ferreira, M. L., Mulitza, S., et al. (2016). Deep water provenance and dynamics of the (de)glacial Atlantic meridional overturning circulation. *Earth and Planetary Science Letters*, *445*, 68–78. https://doi.org/10.1016/j.epsl.2016.04.013

McManus, J. F., Francois, R., Gherardi, J.-M., Keigwin, L. D., & Brown-Leger, S. (2004). Collapse and rapid resumption of Atlantic meridional circulation linked to deglacial climate changes. *Nature*, *428*(6985), 834–837.

Mulitza, S., Chiessi, C., Schefuß, M., Lippold, E., Wichmann, J., Antz, D., et al. (2017). Synchronous and proportional deglacial changes in Atlantic Meridional Overturning and northeast Brazilian precipitation. *Paleoceanography*, *32*, 622–633. https://doi.org/10.1002/2017PA003084

Peterson, L. C., Haug, G. H., Hughen, K. A., & Röhl, U. (2000). Rapid changes in the hydrologic cycle of the tropical Atlantic during the last glacial. *Science*, *290*(5498), 1947–1951.

Pichat, S., Abouchami, W., & Galer, S. J. (2014). Lead isotopes in the Eastern Equatorial Pacific record Quaternary migration of the South Westerlies. *Earth and Planetary Science Letters*, *388*, 293–305.

Pichat, S., Sims, K. W., François, R., McManus, J. F., Brown Leger, S., & Albarède, F. (2004). Lower export production during glacial periods in the equatorial Pacific derived from $(^{231}Pa/^{230}Th)_{xs,\,0}$ measurements in deep-sea sediments. *Paleoceanography*, *19*, PA4023. https://doi.org/10.1029/2003PA000994

Ramsey, C. B. (2009). Bayesian analysis of radiocarbon dates. *Radiocarbon*, *51*(1), 337–360.

Rasmussen, S. O., Andersen, K. K., Svensson, A., Steffensen, J. P., Vinther, B. M., Clausen, H. B., et al. (2006). A new Greenland ice core chronology for the last glacial termination. *Journal of Geophysical Research*, *111*, D06102. https://doi.org/10.1029/2005JD006079

Reimer, P. J., Bard, E., Bayliss, A., Beck, J. W., Blackwell, P. G., Ramsey, C. B., et al. (2013). IntCal13 and Marine13 radiocarbon age calibration curves 0–50,000 years cal BP. *Radiocarbon*, *55*(4), 1869–1887.

Robinson, L. F., Henderson, G. M., Hall, L., & Matthews, I. (2004). Climatic control of riverine and seawater uranium-isotope ratios. *Science*, *305*(5685), 851–854. https://doi.org/10.1126/science.1099673

Svensson, A., Andersen, K. K., Bigler, M., Clausen, H. B., Dahl-Jensen, D., Davies, S. M., et al. (2006). The Greenland ice core chronology 2005, 15–42 ka. Part 2: Comparison to other records. *Quaternary Science Reviews*, *25*(23–24), 3258–3267.

Therón, R., Paillard, D., Cortijo, E., Flores, J.-A., Vaquero, M., Sierro, F. J., et al. (2004). Rapid reconstruction of paleoenvironmental features using a new multiplatform program. *Micropaleontology*, *50*(4), 391–395.

Thomson, J., Nixon, S., Summerhayes, C. P., Schönfeld, J., Zahn, R., & Grootes, P. (1999). Implications for sedimentation changes on the Iberian margin over the last two glacial/interglacial transitions from $(^{230}Th_{excess})_0$ systematics. *Earth and Planetary Science Letters*, *165*(3–4), 255–270. https://doi.org/10.1016/S0012-821X(98)00265-9

Veiga-Pires, C. C., & Hillaire-Marcel, C. (1999). U and Th isotope constraints on the duration of Heinrich events H0-H4 in the southeastern Labrador Sea. *Paleoceanography*, *14*(2), 187–199. https://doi.org/10.1029/1998PA900003

Vidal, L., Labeyrie, L., Cortijo, E., Arnold, M., Duplessy, J., Michel, E., et al. (1997). Evidence for changes in the North Atlantic Deep Water linked to meltwater surges during the Heinrich events. *Earth and Planetary Science Letters*, *146*(1–2), 13–27.

Vinther, B. M., Clausen, H. B., Johnsen, S. J., Rasmussen, S. O., Andersen, K. K., Buchardt, S. L., et al. (2006). A synchronized dating of three Greenland ice cores throughout the Holocene. *Journal of Geophysical Research*, *111*, D13102. https://doi.org/10.1029/2005JD006921

Voelker, A. H. (2002). Global distribution of centennial-scale records for Marine Isotope Stage (MIS) 3: A database. *Quaternary Science Reviews*, *21*(10), 1185–1212.

Wacker, L., Fahrni, S., Hajdas, I., Molnar, M., Synal, H.-A., Szidat, S., et al. (2013). A versatile gas interface for routine radiocarbon analysis with a gas ion source. *Nuclear Instruments and Methods in Physics Research Section B*, *294*, 315–319.

Waelbroeck, C., Duplessy, J.-C., Michel, E., Labeyrie, L., Paillard, D., & Duprat, J. (2001). The timing of the last deglaciation in North Atlantic climate records. *Nature*, *413*(6855), 548.

Waelbroeck, C., Labeyrie, L., Duplessy, J. C., Guiot, J., Labracherie, M., Leclaire, H., et al. (1998). Improving past sea surface temperature estimates based on planktonic fossil faunas. *Paleoceanography*, *13*(3), 272–283. https://doi.org/10.1029/98PA00071

Walter, H., Van der Loeff, M. R., & Hoeltzen, H. (1997). Enhanced scavenging of ^{231}Pa relative to ^{230}Th in the South Atlantic south of the Polar Front: Implications for the use of the ^{231}Pa/^{230}Th ratio as a paleoproductivity proxy. *Earth and Planetary Science Letters*, *149*(1–4), 85–100.

Winckler, G., Anderson, R. F., Jaccard, S. L., & Marcantonio, F. (2016). Ocean dynamics, not dust, have controlled equatorial Pacific productivity over the past 500,000 years. *Proceedings of the National Academy of Sciences of the United States of America*, *113*(22), 6119–6124. https://doi.org/10.1073/pnas.1600616113

Yu, E.-F., Francois, R., & Bacon, M. P. (1996). Similar rates of modern and last-glacial ocean thermohaline circulation inferred. *Nature*, *379*(6567), 689–694.